International Research Journal of Engineering and Technology (IRJET) e-ISSN: 2395 -0056
Volume: 03 Issue: 11 | Nov -2016 www.irjet.net p-ISSN: 2395-0072

Studies on removal of Bromo Phenol Blue dye using Sargassum Muticum powder and Optimization using Central Composite Design

Dr Ch A I Raju[1], K Satyanandam[2]

[1] *chairaju@gmail.com*
Senior Assistant Professor, Department of Chemical Engineering, Andhra University
[2] *k.satyanandam@gmail.com*
Research scholar, Department of Chemical Engineering, Andhra University
Visakhapatnam Andhra Pradesh INDIA 530003

Abstract - *The never ending demand for the process industry like textile, paints and pigments have been of major concern now a days, due to the increased fraction of dyes pollution. The extraction of the above pollution can only be solved using biosorption. Hence an attempt is made using sargarrsum muticum (brown algae) powder for the removal of bromo phenol blue dye. The variables incorporated are time of agitation, biosorbent size, pH, initial concentration, dosage of biosorbent and temperature. The entire experiment process have followed lagengren first order kinetics and langmuir isotherm. The option pH was obtained at 4. The variation of temperature has been found to be increasing up to a certain limit and then after attainable equilibrium, it remained constant. The total experimentation was carried out in a batch process*

Key Words: biosorption, kinetics, isotherms, thermodynamics, brown algae

1. INTRODUCTION

Life on earth without water is impossible, inevitable and inexorable. Water is a prominent and promising barrier for ecological balance. Water is crucial to life for humans or mankind, organisms etc on earth. Worldwide water distribution scenario shows that only 2 % belongs to fresh water and the remaining comprises salt water only **[1, 2]**. As the human race is being acquainted with the advantages of technology, the growth of industrial sector has also enhanced, which inturn increased the pollution. Textile industries have grown hastily due to the increased population and their basic needs like clothing. The final waste from these textile industries is more tough to cleanse completely and the left over is released on to the surface of earth. These pollutants were being settled slowly and polluting the earth's surface and depleting the ground water quality [3]. Drinking or potable water is being associated with these kind of dyes from underground water and humans consuming this contaminated water are being acquainted to new diseases. This can be stopped and eradicated using different techniques [4, 5]. After surveillance of different methods which are expensive and leaves harmful chemicals, Biosorption has been very promising now a days to treat and solve the above problem [6, 7]. With less expensive and naturally available biosorbents the above method is very promising and propitious to solve the textile effluent problems.

2. MATERIALS AND METHODS

The materials and methods consists of the following steps: Reagents and materials, Preparation of the biosorbents and Studies on equilibrium biosorption process.

2.1 Reagents and materials:

All the chemicals used in this investigation were of analytical grade and used without further purification. BPB was used as the source of dye and all the solutions were made with distilled water. The solution of BPB dye was made from a stock solution containing 1000 mg of BPB dye in 1litre. The pH of dye solution was adjusted to the desired value by addition of 0.1M HCL and 0.1M NaOH solutions.

2.2 Preparation of the Biosorbent:

sargarrsum muticum algae was collected from Tenneti Park, Jodugullapalem beach in Visakhapatnam and was washed with water to remove dust and soluble impurities and dried in sun light till the algae became crispy and colorless. The dried algae were finely powdered and sized by passing it through a set of sieves ranging from 300 to 75 mesh sizes. The powder of 53, 75, 105, 125 and 152 micron meters were separated and stored in dry bottles with double cap and used as biosorbent.

2.3 Studies on equilibrium biosorption process:

The biosorption was carried out in a batch process by adding a pre-weighed amount of the *sargarrsum muticum a*lgae powder to a known volume of aqueous solution for a predetermined time interval in an orbital shaker. The procedures adopted to evaluate the effects of various parameters via. Agitation time, pH, initial concentration, biosorbent dosage and temperature of the aqueous solution on the biosorption of BPB dye were evaluated using single step optimization process. Further optimized and checked using Central Composite Design.

3. RESULTS AND DISCUSSION

3.1 Characterization:

3.1.1 FTIR spectrum of untreated Bromo Phenol Blue dye:

FTIR spectrum of untreated Sargassum muticum powder is presented in fig. 1 (a). The sharp peak at 895.01 cm-1 denotes the involvement and participation of S=O and C–S–O from ester sulphonate in biosorption. The bands at 1039.68 and 1056.07 cm-1 indicates the involvement of C–H bending bonds. The bands at 1153.48 cm-1 assigns the C–O stretching bond.

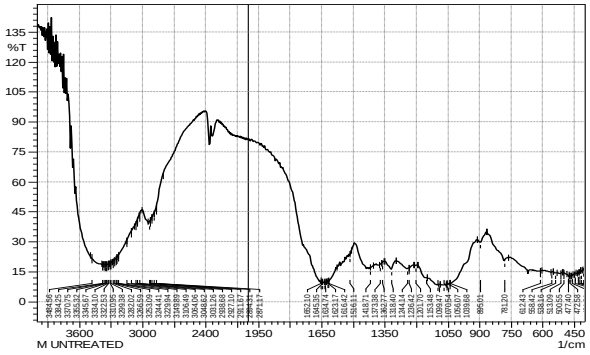

Fig. 1 (a) FTIR spectrum of Bromo Phenol Blue untreated Sargassum muticum powder

The peak at 1201.70 and 1236.42 cm−1 in native biomass designates the presence of C-O stretching, –SO3 stretching bonds and is not observed after loading Bromo Phenol Blue. It indicates the direct involvement of C-O stretching in the ion-exchange process. The bands from 1318.40 to 1373.38 cm-1 denotes the presence of –CH2 bending vibrations. The peaks at 1616.42 and 1623.17 represents the stretching of C=C aromatic rings. The peaks at 1634.74 depict the oleifinic C = C and carbonyl C= O stretching bonds. The peak at 2938.68 cm-1 assigned for CH2 stretching vibrations in is shown in untreated powder. The sharp peak at 3253.09 cm-1 denots the presence of C–H stretching vibrations. Further, the band peaks at 3322.53, 3334.10, 3345.67 and 3355.32 cm-1 are assigned for the bounded –OH and –NH groups and –OH stretching or NH2 stretching bonds.

3.1.2 FTIR spectrum of Bromo Phenol Blue treated with Sargassum muticum powder:

FTIR measurements for Bromo Phenol Blue loaded algal biomass are shown in fig. 1 (b). The sharp peak at 1234.50 cm-1 is shifted to 1236.42 cm-1 denoting the involvement and participation of SO3 streching in biosorption. The shifting of band from 1602.91 cm-1 to 1616.42 cm-1 indicates the involvement of streching of C=C aromatic rings. The bands at 3177.86, 3198.11 and 3209.69 cm-1 (assigned for the presence of C–H stretching vibrations respectively) are not shown in untreated biomass. The characteristic of stretching modes of O–H (indicated by the band at 3312.88 cm-1) is also not seen in untreated biomass.

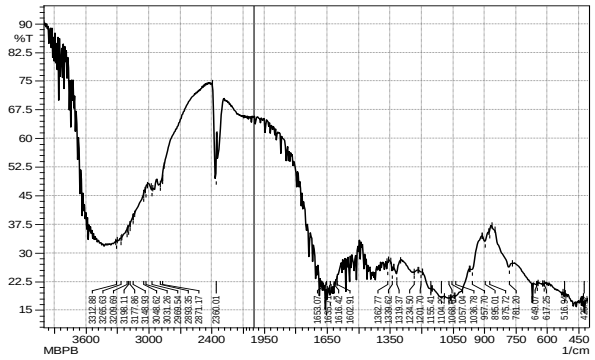

Fig. 1 (b) FTIR spectrum of Bromo Phenol Blue treated Sargassum muticum powder

Table-1

Shift of FTIR peaks for untreated and Sargassum muticum powder treated Bromo Phenol Blue dye

S. No.	Peaks in untreated powder, cm^{-1}	Peaks in treated powder, cm^{-1}	Description
1	---------	425.32	Furan 1,4 cyclooctateraene ring breathing in phase
2	472.58	---------	1,4 swinging in-plane
3	477.40	---------	Weak benzene ring deformation
4	500.55	---------	1,3 and 2,4 symmetric deformation out of phase cyclooctateraene ring deformation
5	513.09	---------	2,4 benzene asymmetric deformation
6	---------	516.94	2,4 benzene asymmetric deformation
7	528.16	---------	2,4 benzene asymmetric deformation
8	558.42	---------	2,4 benzene asymmetric deformation
9	612.43	---------	2,4 benzene deformation out of phase
10	---------	617.25	2,4 benzene deformation out of phase
11	---------	649.07	Weak benzene ring deformation
12	781.20	781.20	Weak benzene ring deformation
13	---------	875.72	S = O and C–S–O bands from ester sulphonate
14	895.01	895.01	S = O and C–S–O bands

			from ester sulphonate
15	---------	957.70	S = O and S–O stretching bond
16	---------	1036.78	C–H bending vibrations
17	1039.68	---------	C–H bending vibrations
18	1056.07	---------	C–H bending vibrations
19	---------	1057.04	C–H bending vibrations
20	---------	1068.61	C–H bending vibrations
21	1070.54	---------	–C–O benzene ring stretching
22	1099.47	---------	–C–O benzene ring stretching
23	---------	1104.29	C–O stretching
24	1153.48	---------	C–O stretching
25	---------	1155.41	C–O stretching
26	1201.70	1201.70	C–O stretching
27	---------	1234.50	-SO_3 stretching
28	1236.42	---------	-SO_3 stretching
29	1244.14	---------	-SO_3 stretching
30	1318.40	---------	–CH_2 bending vibrations
31	---------	1319.37	–CH_2 bending vibrations
32	---------	1339.62	–CH_2 bending vibrations
33	---------	1362.71	–CH_2 bending vibrations
34	1362.77	---------	–CH_2 bending vibrations
35	1373.38	---------	–CH_2 bending vibrations
36	1418.71	---------	C–N stretching
37	1516.11	---------	Amide N–H bending vibrations
38	---------	1602.91	Stretching of C = C aromatic rings
39	1616.42	1616.42	Stretching of C = C aromatic rings
40	1623.17	---------	Stretching of C = C aromatic rings
41	1634.74	---------	Oleifinic C = C and Carbonyl C = O stretching
42	---------	1635.71	Oleifinic C = C and Carbonyl C = O stretching
43	1645.35	---------	Oleifinic C = C and Carbonyl C = O stretching
44	1652.10	---------	Oleifinic C = C and Carbonyl C = O stretching
45	---------	1653.07	Assymetric stretching vibration of C = O
46	---------	2360.01	C ≡ N in the polyacrylnitrile
47	2871.17	2871.17	C–H-stretching
48	---------	2893.35	CH_2 stretching vibrations
49	2894.31	---------	CH_2 stretching vibrations
50	2911.67	---------	CH_2 stretching vibrations
51	2927.10	---------	CH_2 stretching vibrations
52	2938.68	---------	CH_2 stretching vibrations
53	---------	2969.54	CH_2 stretching vibrations
54	3031.26	3031.26	C-H-stretching vibrations
55	3048.62	3048.62	C-H-stretching vibrations
56	3064.06	---------	C-H-stretching vibrations
57	3106.49	---------	C-H-stretching vibrations
58	---------	3148.93	C-H-stretching vibrations
59	3149.89	---------	C-H-stretching vibrations
60	---------	3177.86	C-H-stretching vibrations
61	---------	3198.11	C-H-stretching vibrations
62	---------	3209.69	C-H-stretching vibrations
63	3229.94	---------	C-H-stretching vibrations
64	3244.41	---------	C-H-stretching vibrations
65	3253.09	---------	C-H-stretching vibrations
66	---------	3265.63	C-H-stretching vibrations
67	3266.59	---------	C-H-stretching vibrations
68	3282.02	---------	C-H-stretching vibrations
69	3299.38	---------	C-H-stretching vibrations
70	3310.95	---------	O-H-stretching modes
71	---------	3312.88	O-H-stretching modes
72	3322.53	---------	Bounded –OH and –NH groups
73	3334.10	---------	Bounded –OH and –NH groups
74	3345.67	---------	–OH stretching or –NH_2 stretching
75	3355.32	---------	–OH stretching or –NH_2 stretching
76	3370.75	---------	Hydroxyl stretching or amine stretching
77	3384.25	---------	O-H-stretching modes
78	3484.56	---------	O-H-stretching modes

The sharp peaks of 1010.70 and 1070.49 cm^{-1} arose suddenly after loading of Bromo Phenol Blue due to the involvement of C–O stretching of alcohols and carboxylic acids and –C–O benzene ring stretching respectively. Further, three additional peaks at 1471.69, 1506.41 and 1521.84 cm^{-1} denoting stretching of C=C aromatic rings and 1568.13 cm^{-1} for amide N-H bending vibrations have suddenly appeared in Bromo Phenol Blue treated biomass. The peak appearing at 2343.51 cm^{-1} in Bromo Phenol Blue treated powder is denoting phosphate ester group and is not seen in native biomass. The peaks at 3523.95 and 3566.38 cm^{-1} are obtained in treated biomass due to the involvement of the stretching vibration bands of hydroxyl group. This may be due to the adjustment of pH and physical disruption of cell walls upon the vigorous shaking.

3.1.3 X-Ray Diffraction:

The X-Ray Diffractograms (XRD) of the powder samples are taken using a Rigaku Ultima model IV. The diffracted X-ray intensities are recorded as a function of 2α by using copper target (Cu-Kα radiation with wave length, α= 1.5492 A^0) at a scan speed of 2^0/min. XRD patterns are recorded from 3 to 90^0. Different phases of the samples in figs. 2 (a) & 2(b) are identified by comparing a set of'd' values and the corresponding intensities with the standards from the ICDD (International Center for Diffraction Data) files. XRD pattern does not show very sharp and distinct peaks and exhibits more or less amorphous nature **[8-12].** The peaks at 2θ values of 0.8491, 0.8403, 0.7679, 0.9931 and 0.9782 corroborate the presence of $Fe_2H_{474}K_{44}Na_{10}$, $Ce_2H_{124}K_{0.5}N_{13.5}O_{157}P_4W_{34}$, $C_{162}Cl_{20}N_8O_{80}Pd_4Si_2W_{20}$, $Li_{53.33}N_{32}Ti_{10.67}$ and $CaCrO_4$. Their corresponding d-values are 5.8231, 3.3583, 4.6898, 4.0057 and 3.6550 respectively.

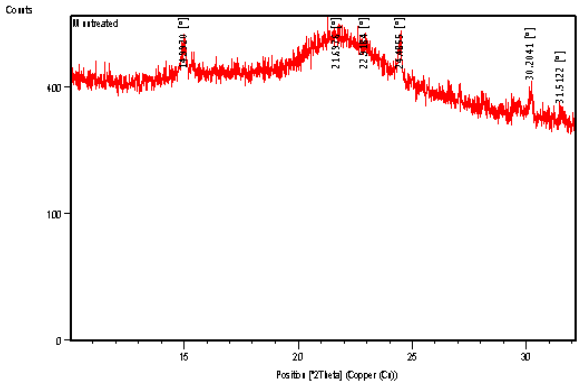

Fig. 2 (a) XRD pattern of Bromo Phenol Blue untreated *Sargassum muticum* powder

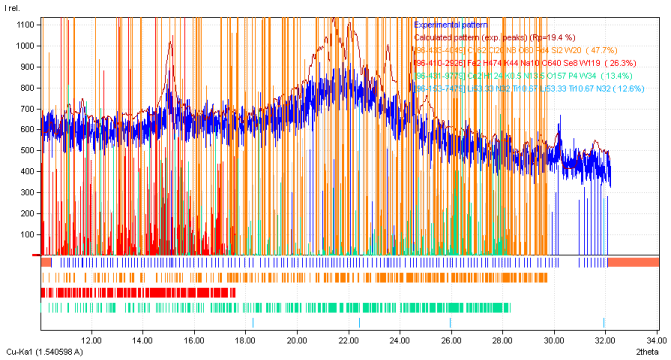

Fig. 2 (b) XRD pattern of Bromo Phenol Blue untreated *Sargassum muticum* powder with matching compounds

XRD patterns of untreated powder are shown in figs. 2 (c) & (d). XRD patterns shown in figs. 2(c) & (d) do not indicate sharp peaks, less crystallinity and exhibit little amorphous nature. The peaks at 2θ values of 0.840, 0.8314, 0.7973, 0.7523 and 0.7090 corroborate the presence of $F_{39}Sb_9Sn_4$, $Ba_8Si_5Sn_4$, $C_{36}I_6N_{12}S_3Zn_3$, $C_{60}S_{16}$ and $AgF_{11}Sb_2$ (ICDD files). Their corresponding d-values are 1.1840, 2.3731, 2.2871, 2.3437 and 1.8213.

3.1.4 XRD for Bromo Phenol Blue dye treated with *Sargassum muticum* powder

XRD patterns for treated powder [Figs. 2(c) & 2(d)] exhibit good crystallinity, more amorphous nature and increase in surface area and porosity. The peaks at 2θ values of 25.597, 11.30, 20.374, 13.421, 12.02, 12.14, 10.029 and 10.963 corroborate the presence of $Sn(HPO_4)_2H_20$, $Cd_3(P_3O_9)_2(H_2O)_{10}$, $Co_5(O_{9.48}H_{8.52})NO_3$, $C_{14}H_8O_2$, $C_6H_{15}CrO_3$, $C_{15}H_{21}CoO_6$ and $Mg_2(Al_4Si_5O_{18})$. Their corresponding d-values are 3.4800, 7.8300, 4.3553, 7.6600, 7.3630, 7.29, 8.82 and 8.07.

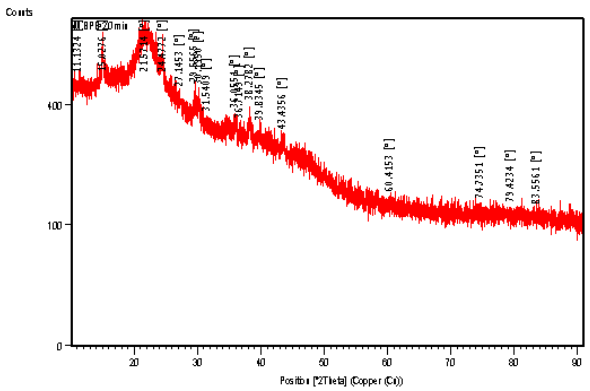

Fig. 2 (c) XRD pattern of Bromo Phenol Blue treated Sargassum muticum powder

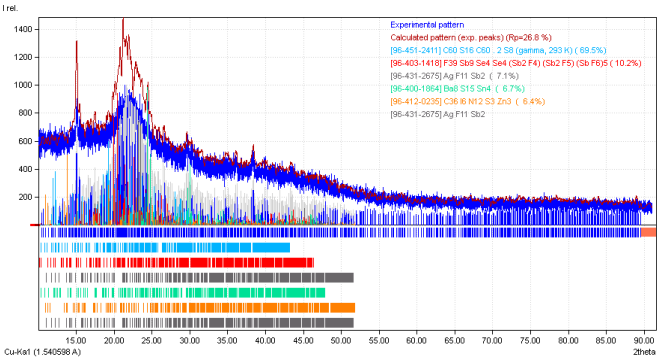

Fig. 2 (d) XRD pattern of Bromo Phenol Blue treated Sargassum muticum powder with matching compounds

3.1.5 Scanning Electron Microscope (SEM):

3.1.3.1 SEM analysis for untreated Sargassum muticum powder

The SEM pictures of untreated sargassum muticum powder shown in fig. 3 (a), demonstrates the surface morphology of powder as porous and uneven. From the SEM images, it is clear that the investigated sorbent is porous material due to the presence of pores and cavities.

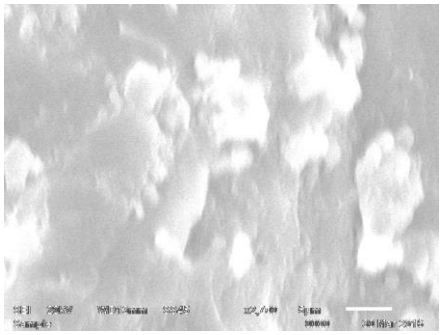

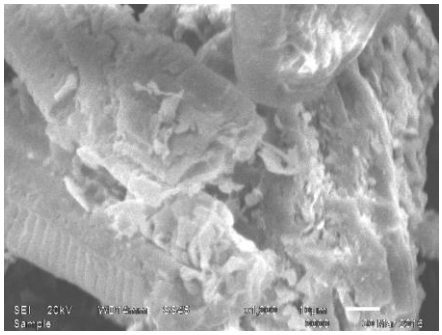

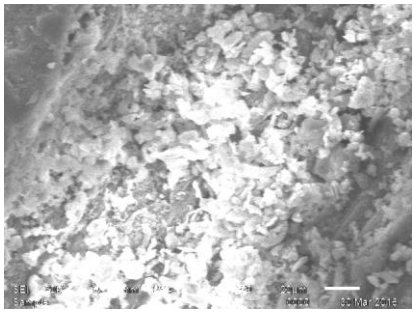

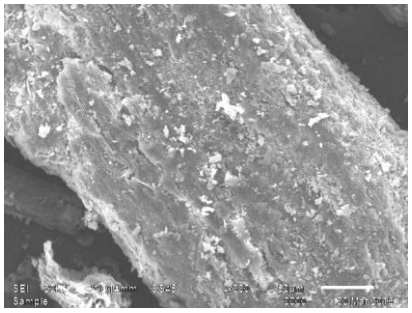

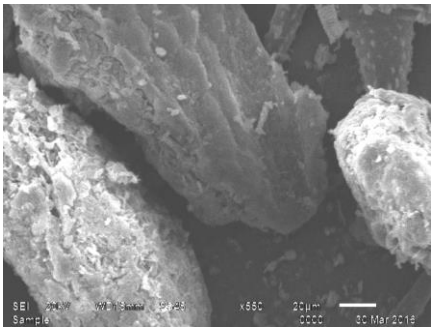

Fig. 3 (a) SEM pattern of Bromo Phenol Blue treated Sargassum muticum powder

3.1.3.2 SEM analysis for Bromo Phenol Blue dye treated with Sargassum muticum powder

SEM analysis after biosorption Fig. 3(b) show that the surface has irregular texture with globular, elongated grains and shiny particles over the surface of cobalt loaded biosorbent which are absent in the fresh biosorbent. These elongated grains show that the cobalt particles are adhered onto the surface of algae. The clustered grains like morphology, on treated biosorbent denote increased active

surface area. The similar results were reported on lead with plant biosorbent, areca catechu powder.

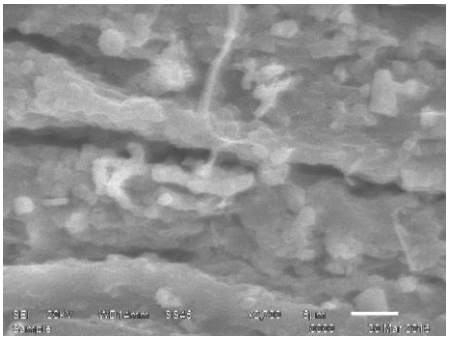

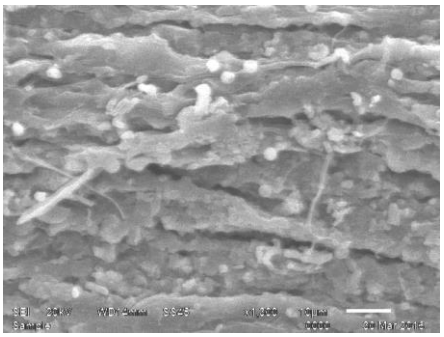

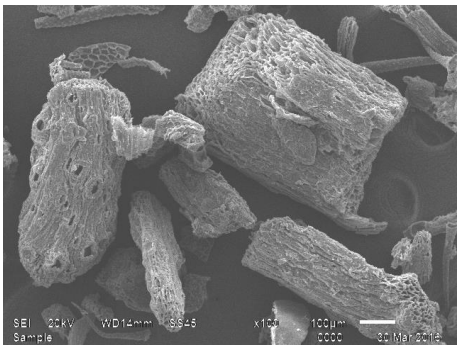

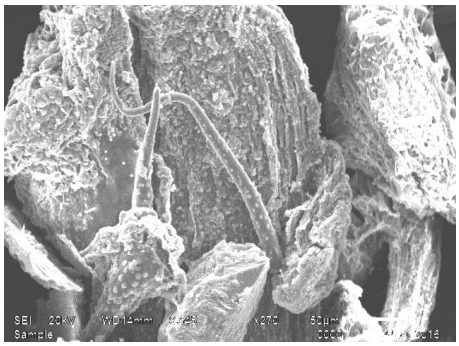

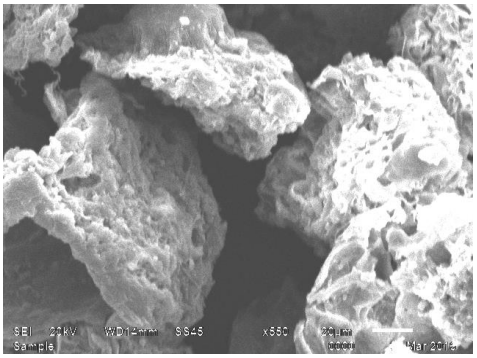

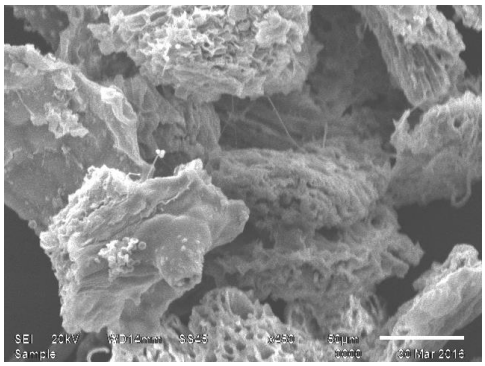

Fig. 3 (b) SEM pattern of Bromo Pheno Blue treated Sargassum muticum powder

3.2 Equilibrium studies on biosorption of Bromo Phenol Blue

3.2.1 Effect of agitation time:

The % biosorption of Bromo Phenol Blue is drawn against agitation time in fig. 4. It is found from the plots that the % biosorption is gradually increased in the first 20 min of agitation. Beyond the agitation time of 20 min, the % biosorption is more or less constant. So the equilibrium agitation time is 20 min. For a typical experiment with 50 mL of aqueous solution adding 10 g/l of 53 µm size biosorbent, the % biosorption is increased from 18 to 65% in the agitation time period of 1 to 20 min. The rate of percentage biosorption is higher in the initial stages because adequate surface area of the biosorbent is available for the biosorption of Bromo Phenol Blue. As time increases, more amount of Bromo Phenol Blue is biosorbed onto the surface of the biosorbent and surface area available decreases **[13-16]**.

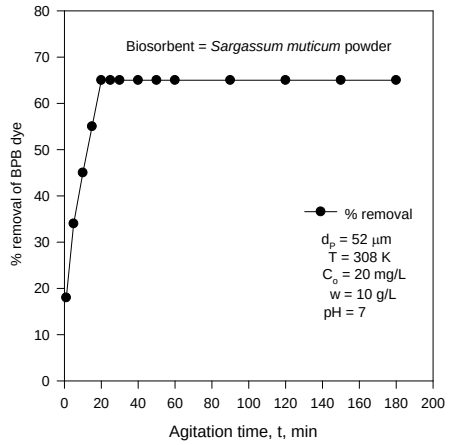

Fig. 4. Effect of agitation time on % biosorption of BPB dye

3.2.2 Effect of biosorbent size:

The variations in % biosorption of Bromo Phenol Blue with biosorbent size are drawn in fig. 5. The percentage biosorption is increased from 45 to 65 % as the biosorbent size decreases from 152 to 53µm. The surface area of the biosorbent increases as the size of the particle decreases and the number of active sites on the biosorbent are better exposed to the biosorbate **[17-21]**.

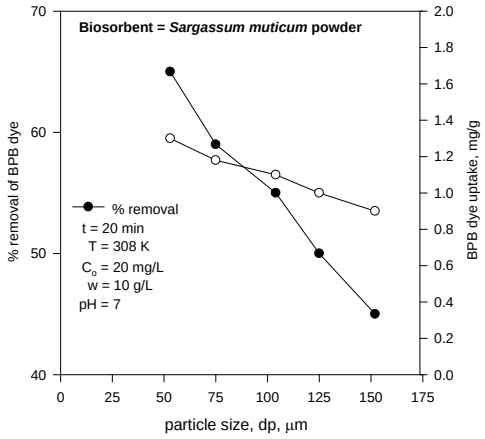

Fig. 5. Effect of biosorbent size on % biosorption

3.2.3 Effect of pH in aqueous solution:

A plot is drawn in fig. 6 between % biosorption of Bromo Phenol Blue and pH of aqueous solution. A significant increase in percentage biosorption of Mn is observed as pH is increased from 2 to 4 and downward trend of the % biosorption is noted with an increase in pH above 4. For a typical experiment with 50 mL of aqueous solution, adding a biosorbent dosage of 10 g/L of 53 µm size, the extent of biosorption is increased from 65 to 86 % in the pH range from 2 to 4. The results indicate that the chemical interactions may have been exchanged between the ions. The carbony, hydroxyl, carbonyl and amide groups of the biomass are mainly involved in the biosorption of Bromo Phenol Blue. Further, presence of -SO3 stretching, S = O and C–S–O bands, from ester sulfonate groups are very rich due to their ion-exchange involvement in biosorption. Similar results were reported for biosorption **[22-26]** of different heavy dyes on various algae species.

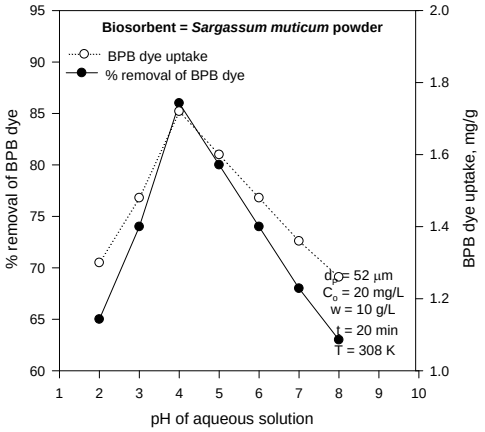

Fig. 6 Effect of pH on % biosorption

3.2.4 Effect of initial concentration of Bromo Phenol Blue:

The effect of initial concentration of Bromo Phenol Blue in the aqueous solution on the percentage biosorption at equilibrium agitation time is shown in fig. 7. The % biosorption is gradually decreased from 86 to 50 % (10 to 1.72 mg/g) by increasing Bromo Phenol Blue Co from 20 to 200 mg/L. Lesser percentage of BPB is removed for higher concentration of BPB in the aqueous solution **[27-31].** This behavior is due to the increase in the amount of biosorbate to the unchanging number of available active sites on the biosorbent.

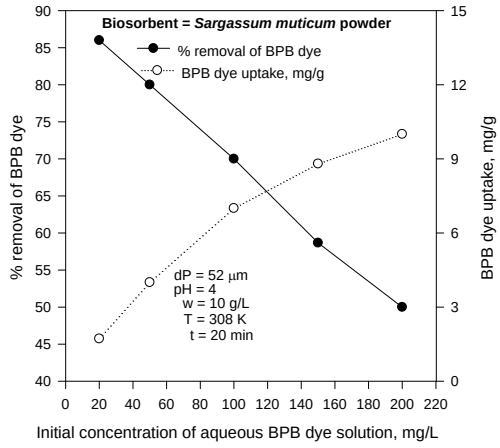

Fig. 7 Effect of initial concentration for the biosorption

3.2.5 Effect of biosorbent dosage:

Fig. 8 represents the variation in percentage biosorption of Bromo Phenol Blue from the aqueous solution (pH = 4) with biosorbent dosage. The % biosorption is increased from 85 to 94% as dosage is increased from 0.5 to 1.5 g/L. The % biosorption from the aqueous phase increases with an increase in the biosorbent amount **[32-35].** This is so

because the number of active sites available for dye uptake would be more as the amount of the biosorbent is increased. The increase in % biosorption is not appreciable (94 to 96.5 %) as w is increased from 1.5 to 4 g/L. All other experiments are conducted at w = 1.5 g/L.

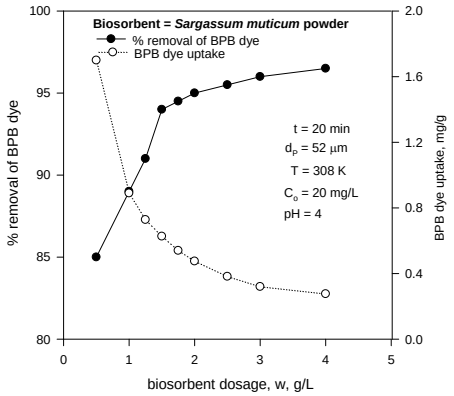

Fig. 8 Effect of biosorbent dosage on % biosorption

3.2.6 Effect of Temperature:

The effect of temperature on the equilibrium dye uptake was significant. The effect of changes in the temperature on the BPB dye uptake is shown in Fig. 9. Results indicate that the adsorption capacity of Saragassum muticum for the BPB red increased with temperature. This may be a result of increase in the mobility of the large dye ion with temperature [36-40]. An increasing number of molecules may also acquire sufficient energy to undergo an interaction with active sites at the surface. Furthermore, increasing temperature may produce a swelling effect within the internal structure of the saragassum muticum enabling large dyes to penetrate further.

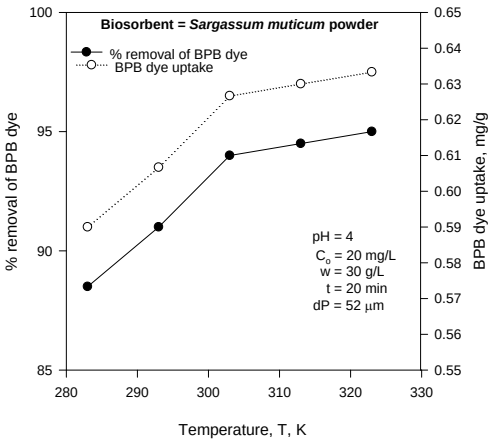

Fig. 9 Effect of temperature for the biosorption

3.2.7 Isotherms:

3.2.7.1 Langmuir Isotherm

Langmuir isotherm is the most widely used simple two-parameter equation. This simple isotherm is based on following assumptions:

- Adsorbate is chemically adsorbed at a fixed number of well- defined sites
- Each site can hold only one adsorbate species
- All sites are energetically equivalent
- There are no interactions between the adsorbate species

The Langmuir relationship is hyperbolic and the equation is:

$$q_e/q_m = K_L C_e / (1+K_L C_e)$$

The above equation can be rearranged as

$$(C_e/q_e) = 1/(K_L q_m) + C_e/q_m$$

From the plots between (C_e/q_e) and C_e, the slope $\{1/(K_L q_m)\}$ and the intercept $(1/q_m)$ can be calculated. Further analysis of Langmuir equation can be made on the basis of separation factor $[R_L = 1/(1+K_L C_e)]$.

Langmuir isotherm is drawn between Ce/qe and Ce in fig. 10 for the present data. The resulting equation is

(Ce/qe) = 0.0854 Ce + 1.5926

The (correlation coefficient of 0.9977) confirms strong binding of Bromo Phenol Blue ions to the surface of *Sargassum muticum* powder.

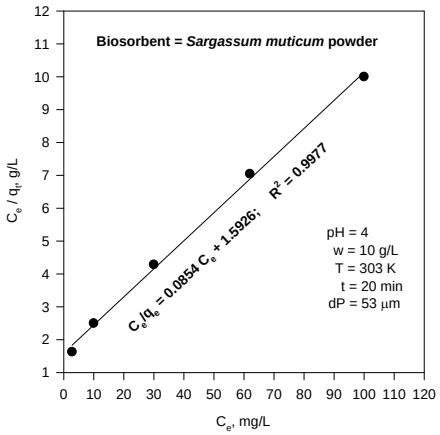

Fig. 10 Langmuir isotherm for biosorption

3.2.7.2 Freundlich isotherm:

Freundlich presented an empirical adsorption isotherm equation that can be applied in case of low and intermediate concentration ranges. The Freundlich isotherm is given by

$q_e = K_f C_e^n$ where Kf, mg/g represents the adsorption capacity at dye equilibrium concentration and n represents the degree of dependence of adsorption.
Taking ln on both sides, we get

$$\ln q_e = \ln K_f + n \ln C_e$$

Freundlich isotherm, drawn between ln Ce and ln qe in fig. 11 has resulted in the following equation
ln qe = 0.4937 ln Ce + 0.1431

The equation has a correlation coefficient of 0.9752. The 'n' value of 0.600508 indicates favorable biosorption satisfying the condition of 0<n<1.

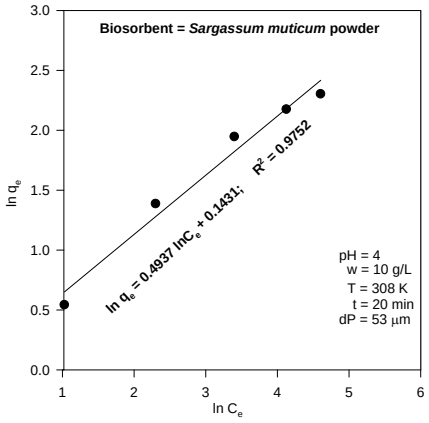

Fig. 11 Freundlich isotherm for biosorption

3.2.7.3 Temkin isotherm:

Temkin and Pyzhev isotherm equation describes the behavior of many adsorption systems on heterogeneous surface and is based on the equation:
qe=RT ln(ATCe)/bT
The linear form of Temkin isotherm is
qe = (RT/ bT) ln(AT) + (RT/bT) ln(Ce)
Where AT= exp [b (0) x b (1) / RT]
Slope, b (1) = RT/ bT
Intercept, b (0) = (RT/ bT) ln (AT)
Plot between qe and ln Ce is shown in fig. 12. The equation for Bromo Phenol Blue biosorption is
qe = 2.3597 ln Ce – 0.9949

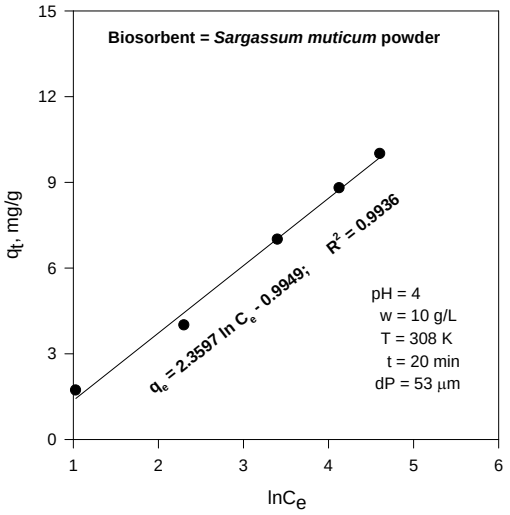

Fig. 12 Temkin isotherm for biosorption

The isotherm constants are compiled in table-5.2. It is found that biosorption data are well represented by Langmuir isotherm (R2=0.9977), Temkin (R2=0.9936) and Freundlich isotherms (R2=0.9752) **[41-46]**.

Table - 2

Isotherm constants (linear method)

Langmuir isotherm	Freundlich isotherm	Temkin isotherm
qm = 11.7096 mg/g	Kf = 1.153845 mg/g	AT = 0.655982 L/mg
KL = 0.053623	n = 0.600508	bT = 1085.185
R2 = 0.9977	R2 = 0.9752	R2 = 0.9936

3.2.8 Kinetics

Lagergren plot and pseudo second order kinetics plot for biosorption of Bromo Phenol Blue are drawn in figs. 13 & 14. Table-3 summarizes the rate constant values for first and second order rate equations **[47-51]**. It is noted that both first and second order rate equationsexplain the biosorption interactions satisfactorily.

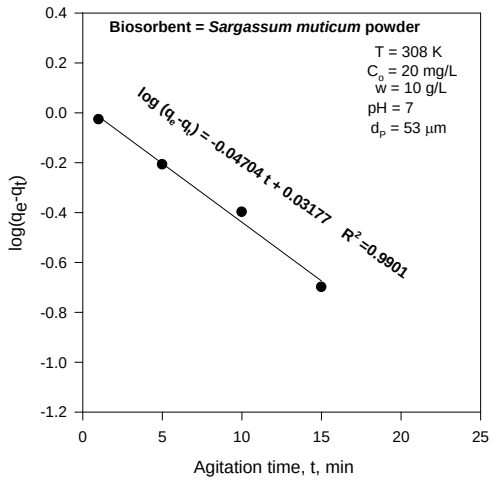

Fig.13 First order kinetics for biosorption

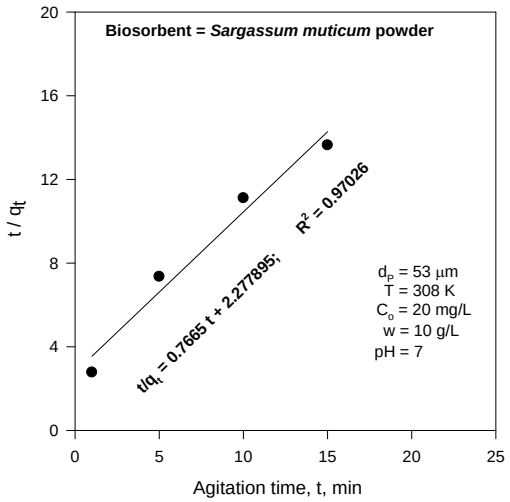

Fig.14 Second order Kinetics for biosorption

Table – 3

Equations and rate constants

Order	Equation	Rate constant	R^2
Lagergren first order	$\log (q_e-q_t) = -0.04704\ t - 0.03177$	0.108333 min^{-1}	0.9901
Pseudo second order	$t/q_t = 0.7665\ t + 2.77895$	0.211419 g/ (mg-min)	0.97026

3.2.9 Thermodynamics:

Van't Hoff's plot is drawn in fig. 15. From the data, Gibbs free energy change (ΔG) is calculated to be –15875 J/mol for biosorption of Bromo Phenol Blue. The negative ΔG value indicates thermodynamically feasible and spontaneous nature of biosorption. The ΔH parameter is 17.92575 kJ/mol.K. The negative ΔH indicates the exothermic nature of biosorption. ΔS parameter is found to be 52.45206 J/mol K for Bromo Phenol Blue biosorption **[52-55]**. The positive ΔS value suggests an increase in the randomness at the solid /solution interface during biosorption.

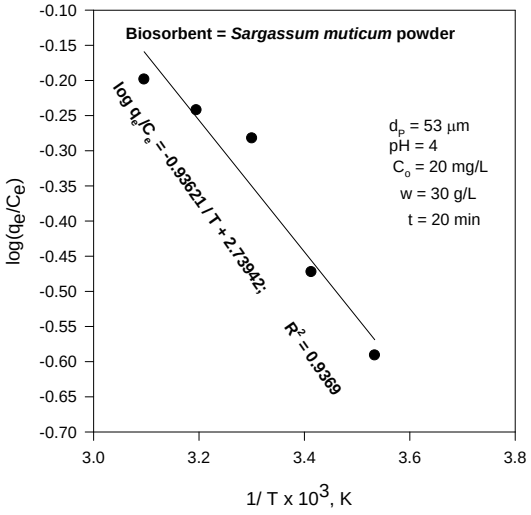

Fig.15 Vant Hoff's plot for biosorption

3.2.10 Optimization using Response Surface Methodology (RSM):

3.2.10.1 Optimization using CCD

The parameters that have greater influence over the response are to be identified so as to find the optimum condition for the biosorption of Bromo Phenol Blue ions. The quadratic model is used in the present study, to relate four independent variables and percentage biosorption of Bromo Phenol Blue. The regression equation for is % biosorption of Bromo Phenol Blue (Y) is function of pH (X1), Co (X3), w (X2) and T (X4)[223-246].

The variations in the corresponding coded values of four parameters and response are presented in table-4

Table-4

Levels of different process variables in coded and un-coded form for % biosorption of Bromo Phenol Blue using Sargassum muticum powder

Var	Name	Range and levels				
		-2	-1	0	1	2
X1	pH	2	3	4	5	6
X2	Initial conc	10	15	20	25	30
X3	Dosag	20	25	30	35	40
X4	Temp	283	293	303	313	323

The following equation represents multiple regression analysis of the experimental data for the biosorption of Bromo Phenol Blue:

$$Y = -1364.39 + 37.32\,X_1 + 2.39\,X_2 + 4.23\,X_3 + 8.49\,X_4 - 4.53\,X_1^2 - 0.06\,X_2^2 - 0.07\,X_3^2 - 0.01\,X_4^2 + 0.00\,X_1X_2 - 0.01\,X_1X_3 - 0.00\,X_1X_4 + 0.00\,X_2X_3 - 0.00\,X_2X_4 + 0.00\,X_3X_4$$

Table-5
Results from CCD for Bromo Phenol Blue biosorption by Sargassum muticum powder

Run no.	X1	X2	X3	X4	% biosorption of Bromo Phenol Blue	
					Experimental	Predicted
1	3	15	25	293	85.98	86.01
2	3	15	25	313	87.50	87.48
3	3	15	35	293	88.08	88.07
4	3	15	35	313	89.58	89.56
5	3	25	25	293	84.08	84.09
6	3	25	25	313	85.52	85.50
7	3	25	35	293	86.52	86.50
8	3	25	35	313	87.90	87.93
9	5	15	25	293	86.40	86.38
10	5	15	25	313	87.78	87.79
11	5	15	35	293	88.18	88.19
12	5	15	35	313	89.62	89.61
13	5	25	25	293	84.48	84.49
14	5	25	25	313	85.80	85.82
15	5	25	35	293	86.62	86.64
16	5	25	35	313	88.02	87.99
17	2	20	30	303	77.86	77.85
18	6	20	30	303	78.32	78.30
19	4	10	30	303	91.58	91.58
20	4	30	30	303	88.08	88.05
21	4	20	20	303	87.36	87.34
22	4	20	40	303	91.58	91.57
23	4	20	30	283	89.28	89.25
24	4	20	30	323	92.08	92.08
25	4	20	30	303	96.22	96.22
26	4	20	30	303	96.22	96.22
27	4	20	30	303	96.22	96.22
28	4	20	30	303	96.22	96.22
29	4	20	30	303	96.22	96.22
30	4	20	30	303	96.22	96.22

Experimental conditions [Coded Values] and observed response values of central composite design with 2^4 factorial runs, 6- central points and 8- axial points. Agitation time fixed at 60 min and biosorbent size at 53 µm

Table- 6 represents the results obtained in CCD. Response obtained from regression in eq. in the form of ANOVA is presented. From the Fisher's F-test (Fmodel = 285.1025) and a very low probability value (Pmodel > F=0.000000), it is known from table–7 that the model is highly significant. At 5% level, the computed F-value (F0.05 (14.15) = MSmodel/MSerror = 285.1025) is greater than that of the tabular F-value (F0.05 (14.15) tabulars = 2.42), indicating that the treatment differences are significant

Table-6
ANOVA of Bromo Phenol Blue biosorption for entire quadratic model

Source of variation	SS	Df	Mean square(MS)	F-value	P > F
Model	120.701	14	8.6215	285.102	0.0000
Error	0.4536	15	0.03024		
Total	121.155				

df- degree of freedom; SS- sum of squares; F- factor F; P-probability
R2=0.99999; R2 (adj):0.99998:

The larger the value of t and smaller the value of P, the more significant is the corresponding coefficient term. The't' and 'P' values are analyzed from table-6.8. It is found that the X1, X2, X3, X4, X12 , X22 , X32 , X42 X1X2, X1X3, X2X3 and X2X4 have high significance to explain the

Table-7 Estimated regression coefficients for the Bromo Phenol Blue biosorption onto Sargassum muticum powder

Terms	Regression coefficient	Standard error of the coefficient	t-value	*P*-value
Mean	-1364.39	4.151	-328.6	0.000
Dosage (L)	37.32	0.175	213.15	0.000

Dosage (Q)	-4.53	0.004	-1076	0.000
Conc, (L)	2.39	0.035	68.25	0.000
Conc, (Q)	-0.06	0.000	-379	0.000
pH (L)	4.23	0.035	119.1	0.000
pH (Q)	-0.07	0.000	-401	0.000
Temp (L)	8.49	0.025	327.4	0.000
Temp (Q)	-0.01	0.000	-329	0.000
1L by 2L	0.00	0.001	0.68	0.506
1L by 3L	-0.01	0.001	-11.5	0.000
1L by 4L	-0.00	0.000	-3.40	0.003
2L by 3L	0.00	0.000	15.64	0.000
2L by 4L	-0.00	0.000	-3.40	0.003
3L by 4L	0.00	0.000	0.68	0.506

[a]insignificant (P ≥ 0.05)

individual and interaction effect of independent variables on Bromo Phenol Blue biosorption. The other terms (X1X2, X1X4, X2X3, X2X4 and X3X4) are insignificant and are not required to explain biosorption. The model is reduced to the following form by removing insignificant terms.

$$Y = -1364.39 + 37.32\,X_1 + 2.39\,X_2 + 4.23\,X_3 + 8.49\,X_4 - 4.53\,X_1^2 - 0.06\,X_2^2 - 0.07\,X_3^2 - 0.01\,X_4^2 - 0.01\,X_1X_3$$

A synergistic effect is indicated by positive sign of the coefficient which means response increases with an increase in effect, while an antagonistic effect is indicated by a negative sign which means response decreases with an increase in effect. In the observed response values, a measure of the models variability is provided by the correlation coefficient (R2). In the present study, the value of the regression coefficient (R2 = 0.9999) for eq. indicates that 0.001 % of the total variations are not satisfactorily explained by the model. It is proved from that table that Fstatistics value for entire model is higher. This large value means that % biosorption can be adequately explained by the model equation. Generally P values lower than 0.05 indicates that the model is considered to be statistically significant at 95% confidence level. The % biosorption prediction from the model is shown in table-6.6. It is implied from table-6.8 that all the squared terms of all the variables and the linear terms are significant (P < 0.05). Among the interaction terms, all the terms (P < 0.05) are insignificant on the biosorption capacity. Fig.5.16 shows normal probability plot (NPP) of residual values. It could be seen that the experimental points are reasonably aligned suggesting normal distribution.

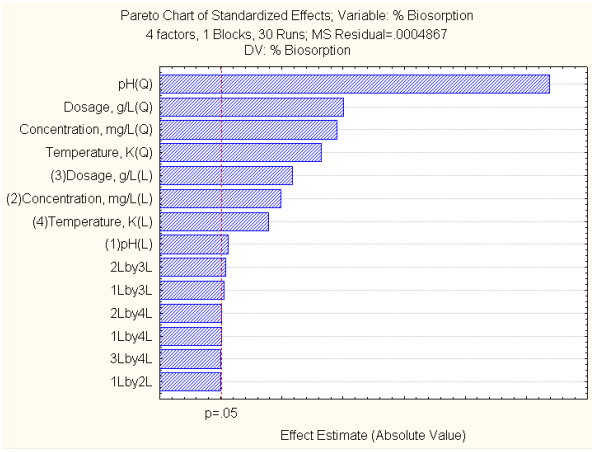

Fig. 16 Pareto Chart

5.6.2 Interaction effects of biosorption variables:

The three-dimensional view of response surface contour plots [Fig. 18 (a) to (f)] show % biosorption as a function of for various combinations of independent variables. The plots are represented as a function of two factors at a time keeping other factors fixed at zero level,.

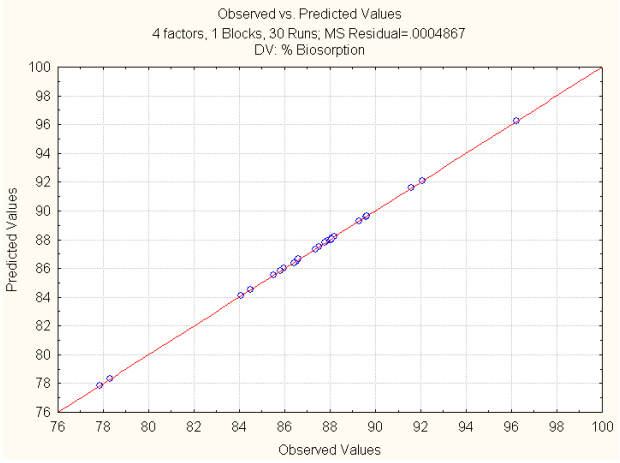

Fig. 17 Normal probability plot for % biosorption of Bromo Phenol Blue

It is found from the response surface plots that the % biosorption is maximal at low and high levels of the input variables. However, there exists a region where neither an increasing nor a decreasing trend in % biosorption is observed. The biosorption variables should be optimum to maximize the % biosorption. The % biosorption of Bromo Phenol Blue is strongly influenced by the pH as evident from figs. 18 (a) & (b).

The predicted optimal set of conditions for percentage biosorption of Bromo Phenol Blue is

pH of aqueous solution = 4.0094
Initial Bromo Phenol Blue dye conc = 18.6548 mg/L
Biosorbent dosage = 31.5332 g/L
Temperature = 305.5716 K
% biosorption of Bromo Phenol Blue = 96.5926

The optimal set of conditions obtained with CCD are shown in table-8 along with experimental values.

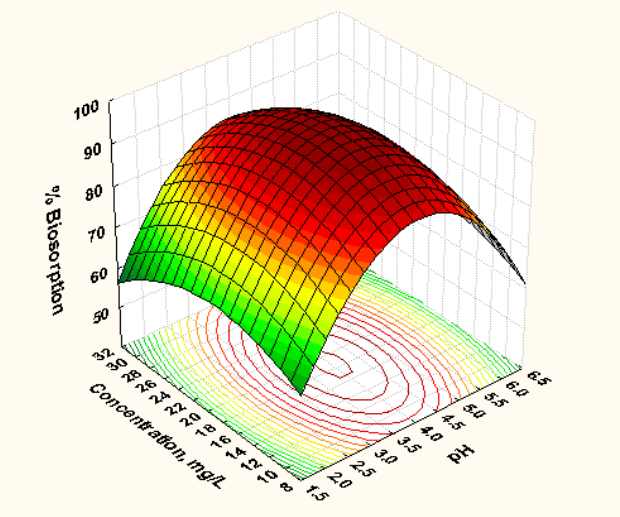

Fig. 18 (a) Surface contour plot for the effects of pH and initial Bromo Phenol Blue concentration on % biosorption

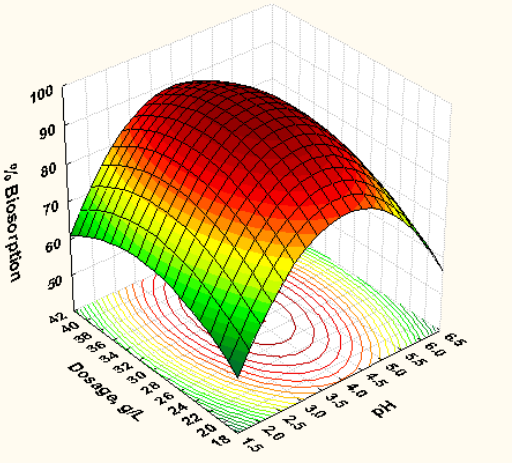

Fig. 18 (b) Surface contour plot for the effects of dosage and pH on % biosorption of Bromo Phenol Blue

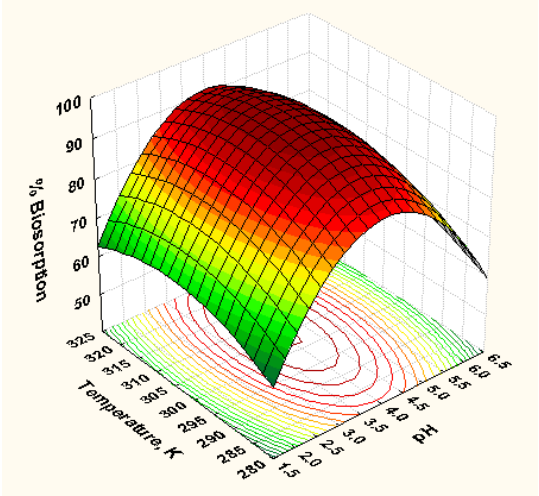

Fig. 18 (c) Surface contour plot for the effects of pH and Temperature on % biosorption of Bromo Phenol Blue

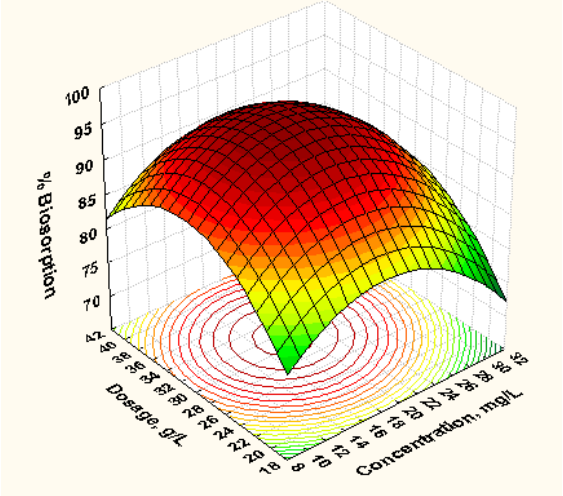

Fig. 18 (d) Surface contour plot for the effects of initial concentration and dosage on % biosorption of Bromo Phenol Blue

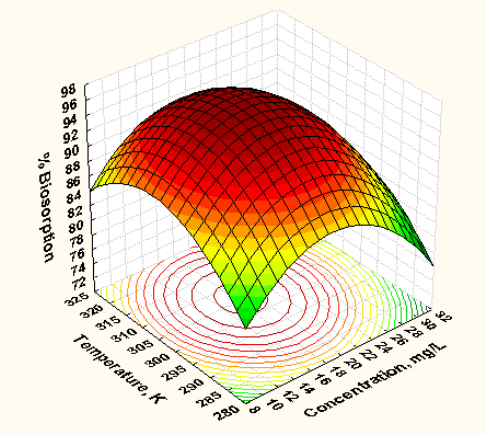

Fig. 18 (e) Surface contour plot for the effects of initial concentration and Temperature on % biosorption of Bromo Phenol Blue

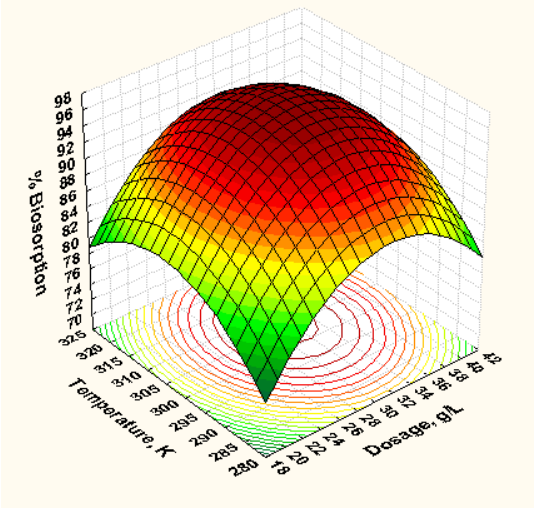

Fig. 18 (f) Surface contour plot for the effects of dosage and Temperature on % biosorption of Bromo Phenol Blue

Table – 8
Comparison between optimum values from CCD and experimentation

Variable	CCD	Exp value
pH of aqueous solution	4.0094	4
Initial BPB dye concentration, mg/L	18.6548	20
Biosorption dosage, w, g/L	31.5332	30
Temperature, K	305.5716	303
% biosorption	96.5926	95.0

Table – 9
Dyes uptake capacities for different biosorbents

Authors	Biosorbent	q_t, mg/g
A. Bennani Karim et al [56]	Moroccan clay	50.25
Barka Noureddine et al [57]	crystalline Hydroxy apatite	243.9
Dong Yanan et al [58]	Activated Carbon	133
Fatih Deniz et al [59]	Paulownia tomentosa Steud. leaf powder	0.57
George Z. Kyzas et al [60]	carbon prepared from rice husk	690
Gonul Akkaya et al [61]	Dicranella varia	2000
Gurusamy Annadurai [62]	Strongly Chelating Polymer chitosan	40
Hema M et al [63]	acid activated low cost carbon	9.5693
Jung-Hyun Kim et al [64]	Polymer Particles	67
M. Santoshkumar et al [65]	native biomass of a new isolate of Penicillium sp	5.88
Present investigation	Sargassum muticum powder	11.7096

CONCLUSIONS

The equilibrium agitation time for BPB dye biosorption is 20 minutes. Percentage biosorption of BPB dye from the aqueous solution increases significantly with increase in pH from 2 (65 %) to 4 (86 %). The optimum dosage for biosorption is 30 g/L (0.6266 mg/g). The maximum uptake capacity of 11.7096 mg/g is obtained at 303 K. The maximum biosorption of BPB dye (96.5926 %) onto Sargassum Muticum powder is observed when the processing parameters are set as: pH = 4.0094, w = 31.5332 g/L, Co = 18.6548 mg/L and T = 305.5716 K using CCD. The thermodynamic data show that % biosorption of BPB dye is increased with increase in temperature. The investigation also reveals the endothermic nature of biosorption as ΔH is positive (17.92575), irreversible nature of biosorption as ΔS is positive (52.45206) and spontaneity of biosorption as indicated by negative ΔG (ΔG = −15875 J/mole). With the above conclusions the authors confirm that sargassum muticum is capable of removing BPB dye.

ACKNOWLEDGEMENT

The authors express their sincere thanks and gratitude to department of chemical engineering, Andhra University for supporting financially (TEQIP) and providing space and experimental facilities. The authors also express their sincere regards to Advanced Analytical Laboratory, Andhra University for helping in studying characterization techniques like FTIR, XRD and SEM.

REFERENCES

[1] Ramachandra T.V., Ahalya N. and Rajasekara Murthy C., (2005) "Aquatic ecosystems: conservation, restoration and management", Capital Publishers, New Delhi.

[2] Ramachandra T.V., Kiran R and Ahalya N (2002) Status, Conservation and Management of Wetlands–– Allied Publishers (P) Ltd, India.

[3] R Sai Ram Seshu and Dipti Kumari, "Water Pollution: A Major Threat to Living Forms", Research and Reviews: Journal of Ecology and Environmental Sciences, RRJEES Volume 3 Issue 1 January - March, 2015

[4] V. Karthik , K. Saravanan , P.Bharathi , V.Dharanya , C.Meiaraj, "An overview of treatments for the removal of

textile dyes", Journal of Chemical and Pharmaceutical Sciences, JCPS Volume 7 Issue 4, October-December 2014, 301–307.

[5] A. El-Maghraby and H.A. El Deeb, "Removal of a Basic Dye From Aqueous Solution by Adsorption Using Rice Hulls", Global NEST Journal, Vol 13, No 1, 2011, pp 90-98.

[6] Mustafa T. Yagub, Tushar Kanti Sen,Sharmeen Afroze and H.M. Ang, "Dye and its removal from aqueous solution by adsorption: A review", Advances in Colloid and Interface Science Volume 209, July 2014, Pages 172–184.

[7] E. Voudrias, K. Fytianos and E. Bozani, "Sorption - Desorption Isotherms of Dyes from Aqueous Solutions and Wastewaters with Different Sorbent Materials", Global Nest: the Int. J. Vol 4, No 1, 2002, pp 75-83.

[8] Allen, P. G., et al. "Investigation of aquo and chloro complexes of UO22+, NpO2+, Np4+, and Pu3+ by X-ray absorption fine structure spectroscopy."Inorganic chemistry 36.21 (1997): 4676-4683.

[9] Bradder, Philip, et al. "Dye adsorption on layered graphite oxide." Journal of Chemical & Engineering Data 56.1 (2010): 138-141.

[10] Burnside, Shelly D., et al. "Self-organization of TiO2 nanoparticles in thin films." Chemistry of materials 10.9 (1998): 2419-2425.

[11] Chen, C. L., X. K. Wang, and M. Nagatsu. "Europium adsorption on multiwall carbon nanotube/iron oxide magnetic composite in the presence of polyacrylic acid." Environmental science & technology 43.7 (2009): 2362-2367.

[12] Chen, Changlun, et al. "Adsorption behavior of multiwall carbon nanotube/iron oxide magnetic composites for Ni (II) and Sr (II)." Journal of hazardous materials 164.2 (2009): 923-928.

[13] Namasivayam C, Kavitha D. Removal of Congo Red from water by adsorption onto activated carbon prepared from coir pith, an agricultural solid waste. Dyes and pigments. 2002 Jul 31; 54(1):47-58.

[14] Garg VK, Gupta R, Yadav AB, Kumar R. Dye removal from aqueous solution by adsorption on treated sawdust. Bioresource Technology. 2003 Sep 30; 89(2):121-4.

[15] Sivaraj R, Namasivayam C, Kadirvelu K. Orange peel as an adsorbent in the removal of acid violet 17 (acid dye) from aqueous solutions. Waste management. 2001 Dec 31; 21(1):105-10.

[16] Kavitha D, Namasivayam C. Experimental and kinetic studies on methylene blue adsorption by coir pith carbon. Bioresource Technology. 2007 Jan 31; 98(1):14-21.

[17] Ho YS, Chiang TH, Hsueh YM. Removal of basic dye from aqueous solution using tree fern as a biosorbent. Process Biochemistry. 2005 Jan 31;40(1):119-24.

[18] Gong R, Ding Y, Li M, Yang C, Liu H, Sun Y. Utilization of powdered peanut hull as biosorbent for removal of anionic dyes from aqueous solution. Dyes and Pigments. 2005 Mar 31;64(3):187-92.

[19] Ho YS, McKay G. A kinetic study of dye sorption by biosorbent waste product pith. Resources, conservation and recycling. 1999 Mar 1;25(3):171-93.

[20] Robinson T, Chandran B, Nigam P. Removal of dyes from a synthetic textile dye effluent by biosorption on apple pomace and wheat straw. Water research. 2002 Jun 30;36(11):2824-30.

[21] Arami M, Limaee NY, Mahmoodi NM. Evaluation of the adsorption kinetics and equilibrium for the potential removal of acid dyes using a biosorbent. Chemical Engineering Journal. 2008 May 15;139(1):2-10.

[22] Janoš P, Buchtová H, Rýznarová M. Sorption of dyes from aqueous solutions onto fly ash. Water research. 2003 Dec 31; 37(20):4938-44.

[23] Annadurai G, Juang RS, Lee DJ. Use of cellulose-based wastes for adsorption of dyes from aqueous solutions. Journal of hazardous materials. 2002 Jun 10; 92(3):263-74.

[24] Malik PK. Use of activated carbons prepared from sawdust and rice-husk for adsorption of acid dyes: a case study of Acid Yellow 36. Dyes and pigments. 2003 Mar 31; 56(3):239-49.

[25] Thangamani KS, Sathishkumar M, Sameena Y, Vennilamani N, Kadirvelu K, Pattabhi S, Yun SE. Utilization of modified silk cotton hull waste as an adsorbent for the removal of textile dye (reactive blue MR) from aqueous solution. Bioresource technology. 2007 Apr 30; 98(6):1265-9.

[26] Chiou MS, Li HY. Adsorption behavior of reactive dye in aqueous solution on chemical cross-linked chitosan beads. Chemosphere. 2003 Mar 31; 50(8):1095-105.

[27] Ho YS, McKay G. Pseudo-second order model for sorption processes. Process biochemistry. 1999 Jul 31; 34(5):451-65.

[28] Lee PC, Meisel D. Adsorption and surface-enhanced Raman of dyes on silver and gold sols. The Journal of Physical Chemistry. 1982 Aug; 86(17):3391-5.

[29] Garg VK, Amita M, Kumar R, Gupta R. Basic dye (methylene blue) removal from simulated wastewater by adsorption using Indian Rosewood sawdust: a timber industry waste. Dyes and pigments. 2004 Dec 31; 63(3):243-50.

[30] Wang S, Li H. Dye adsorption on unburned carbon: kinetics and equilibrium. Journal of hazardous materials. 2005 Nov 11; 126(1):71-7.

[31] Tan IA, Ahmad AL, Hameed BH. Adsorption of basic dye on high-surface-area activated carbon prepared from coconut husk: Equilibrium, kinetic and thermodynamic studies. Journal of Hazardous Materials. 2008 Jun 15; 154(1):337-46.

[32] Akar ST, Gorgulu A, Akar T, Celik S. Decolorization of Reactive Blue 49 contaminated solutions by Capsicum annuum seeds: Batch and continuous mode biosorption applications. Chemical engineering journal. 2011 Mar 15; 168(1):125-33.

[33] Srinivasan A, Viraraghavan T. Decolorization of dye wastewaters by biosorbents: a review. Journal of environmental management. 2010 Oct 31; 91(10):1915-29.

[34] Ncibi MC, Mahjoub B, Seffen M. Kinetic and equilibrium studies of methylene blue biosorption by Posidonia oceanica (L.) fibres. Journal of Hazardous Materials. 2007 Jan 10; 139(2):280-5.

[35] Pavan FA, Lima EC, Dias SL, Mazzocato AC. Methylene blue biosorption from aqueous solutions by yellow passion fruit waste. Journal of hazardous materials. 2008 Feb 11; 150(3):703-12.

[36] Ghosh D, Bhattacharyya KG. Adsorption of methylene blue on kaolinite. Applied Clay Science. 2002 Feb 28;20(6):295-300.

[37] Mittal A. Adsorption kinetics of removal of a toxic dye, Malachite Green, from wastewater by using hen feathers. Journal of hazardous materials. 2006 May 20;133(1):196-202.

[38] Ofomaja AE, Ho YS. Equilibrium sorption of anionic dye from aqueous solution by palm kernel fibre as sorbent. Dyes and Pigments. 2007 Dec 31;74(1):60-6.

[39] Mahmoodi NM, Hayati B, Arami M, Lan C. Adsorption of textile dyes on pine cone from colored wastewater: kinetic, equilibrium and thermodynamic studies. Desalination. 2011 Mar 1;268(1):117-25.

[40] Lee CK, Lin KS, Wu CF, Lyu MD, Lo CC. Effects of synthesis temperature on the microstructures and basic dyes adsorption of titanate nanotubes. Journal of hazardous materials. 2008 Feb 11;150(3):494-503.

[41] Foo 55, Hameed BH. Insights into the modeling of adsorption isotherm systems. Chemical Engineering Journal. 2010 Jan 1;156(1):2-10.

[42] Allen SJ, Mckay G, Porter JF. Adsorption isotherm models for basic dye adsorption by peat in single and binary component systems. Journal of colloid and interface science. 2004 Dec 15;280(2):322-33.

[43] Wong YC, Szeto YS, Cheung W, McKay G. Adsorption of acid dyes on chitosan—equilibrium isotherm analyses. Process Biochemistry. 2004 Feb 25;39(6):695-704.

[44] Vimonses V, Lei S, Jin B, Chow CW, Saint C. Kinetic study and equilibrium isotherm analysis of Congo Red adsorption by clay materials. Chemical Engineering Journal. 2009 May 15;148(2):354-64.

[45] Khaled A, El Nemr A, El-Sikaily A, Abdelwahab O. Removal of Direct N Blue-106 from artificial textile dye effluent using activated carbon from orange peel: Adsorption isotherm and kinetic studies. Journal of Hazardous Materials. 2009 Jun 15;165(1):100-10.

[46] Özcan A, Öncü EM, Özcan AS. Kinetics, isotherm and thermodynamic studies of adsorption of Acid Blue 193 from aqueous solutions onto natural sepiolite. Colloids and Surfaces A: Physicochemical and Engineering Aspects. 2006 Apr 5;277(1):90-7.

[47] Wang L, Zhang J, Zhao R, Li C, Li Y, Zhang C. Adsorption of basic dyes on activated carbon prepared from Polygonum orientale Linn: equilibrium, kinetic and thermodynamic studies. Desalination. 2010 May 15; 254(1):68-74.

[48] Uddin MT, Islam MA, Mahmud S, Rukanuzzaman M. Adsorptive removal of methylene blue by tea waste. Journal of Hazardous Materials. 2009 May 15; 164(1):53-60.

[49] Wang S, Li H. Structure directed reversible adsorption of organic dye on mesoporous silica in aqueous solution. Microporous and mesoporous materials. 2006 Dec 29; 97(1):21-6.

[50] Özcan AS, Erdem B, Özcan A. Adsorption of Acid Blue 193 from aqueous solutions onto BTMA-bentonite. Colloids and Surfaces A: Physicochemical and Engineering Aspects. 2005 Sep 15; 266(1):73-81.

[51] Sureshkumar MV, Namasivayam C. Adsorption behavior of Direct Red 12B and Rhodamine B from water onto surfactant-modified coconut coir pith. Colloids and Surfaces A: Physicochemical and Engineering Aspects. 2008 Mar 20; 317(1):277-83.

[52] Eren, E., and B. Afsin. "Investigation of a basic dye adsorption from aqueous solution onto raw and pre-treated bentonite surfaces." Dyes and Pigments 76.1 (2008): 220-225.

[53] Hameed, B. H., A. A. Ahmad, and N. Aziz. "Isotherms, kinetics and thermodynamics of acid dye adsorption on activated palm ash." Chemical Engineering Journal 133.1 (2007): 195-203.

[54] Wu, Zhijian, Hyeonwoo Joo, and Kangtaek Lee. "Kinetics and thermodynamics of the organic dye adsorption on the mesoporous hybrid xerogel." Chemical Engineering Journal 112.1 (2005): 227-236.

[55] Eren, E., and B. Afsin. "Investigation of a basic dye adsorption from aqueous solution onto raw and pre-treated sepiolite surfaces." Dyes and Pigments 73.2 (2007): 162-167.

[56] Bennani Karim , B. Mounir, M. Hachkar, M. Bakasse and A.Yaacoubi, "Adsorption of Malachite Green dye onto raw Moroccan clay in batch and dynamic system", Canadian Journal on Environmental, Construction and Civil Engineering Vol. 2, No. 2, February 2011

[57] Barka Noureddine, Qourzal Samir, Assabbane Ali, Nounah Abederrahman and Ait-ichou Yhya, "Adsorption of Disperse Blue SBL dye by synthesized poorly crystalline Hydroxyapatite", Journal of Environmental Sciences 20(2008) 1268–1272

[58] Dong Yanan , Su Yanle, Chen Wenjuan , Peng Jinming , Zhang Yan and Jiang Zhongyi, "Ultrafiltration Enhanced with Activated Carbon Adsorption for Efficient Dye Removal from Aqueous Solution", Chinese Journal of Chemical Engineering, 19(5) 863—869 (2011)

[59] Fatih Deniz and Saadet D. Saygideger, "Equilibrium, kinetic and thermodynamic studies of Acid Orange 52 dye biosorption by Paulownia tomentosa Steud. leaf powder as a low-cost natural biosorbent", Bioresource Technology 101 (2010) 5137–5143

[60] George Z. Kyzas , Jie Fu and Kostas A. Matis, "The Change from Past to Future for Adsorbent Materials in Treatment of Dyeing Wastewaters", Materials 2013, 6, 5131-5158

[61] Gonul Akkaya and Ayla Ozer, "Biosorption of Acid Red 274 (AR 274) on Dicranella varia:Determination of equilibrium and kinetic model parameters", Process Biochemistry 40 (2005) 3559–3568

[62] Gurusamy Annadurai , "Adsorption of Basic Dye on Strongly Chelating Polymer: Batch Kinetics Studies", Iranian PolynterJourual / Volume II Number 4 (2002)

[63] Hema M and Arivoli S., "Adsorption kinetics and thermodynamics of malachite green dye unto acid activated low cost carbon", J. Appl. Sci. Environ. Manage. March, 2008 ,Vol. 12(1) 43 – 51

[64] Jung-Hyun Kim and Jeong-Yeol Yoon, "Protein Adsorption on Polymer Particles",

[65] M. Santoshkumar, O. Anjaneya, S. Nayak Anand and T.B. Karegoudar, "Biosorption of acid violet dye from aqueous solutions using native biomass of a new isolate of Penicillium sp.", International Biodeterioration & Biodegradation 63 (2009) 782–787